Isr. J. Earth Sci.; 51: 297–309

Stratigraphic, geochronologic, and paleomagnetic constraints on Late Cretaceous volcanism in northern Israel

Amit Segev,[a] Eytan Sass,[b] Hagai Ron,[b,c] Barbu Lang,[a] Yehoshua Kolodny,[b] and Michael McWilliams[d]

[a]Geological Survey of Israel, 30 Malkhe Yisrael Street, Jerusalem 95501, Israel
[b]Institute of Earth Sciences, The Hebrew University of Jerusalem, Jerusalem 91904, Israel
[c]The Geophysical Institute of Israel, Lod 7110, Israel
[d]Geological and Environmental Sciences, Stanford University, Stanford, California 94305-21215, USA

(Received 13 June 2002; accepted in revised form 10 October 2002)

ABSTRACT

Segev, A., Sass, E., Ron, H., Lang, B., Kolodny, Y., McWilliams, M. 2002. Stratigraphic, geochronologic, and paleomagnetic constraints on Late Cretaceous volcanism in northern Israel. Isr. J. Earth Sci. 51: 297–309.

Late Cretaceous volcanism in northern Israel is represented by basaltic pyroclastics and lavas at two adjacent localities at Mount Carmel and the Umm el Fahm area. Four Cenomanian and one Senonian volcanic intercalation occur in the marine succession. These volcanic rocks were dated by the $^{40}Ar/^{39}Ar$ and K–Ar techniques using whole rock, amphibole megacrysts, and plagioclase fractions. Paleomagnetic measurements were performed on the Senonian pyroclastics.

Amphibole from the oldest Cenomanian volcanic unit in Mount Carmel (the Kerem Maharal pyroclastics, at the base of the Chalk Complex) yielded an age of 97.1 ± 1.7 Ma. The penultimate Cenomanian volcanic unit in Mount Carmel (basalt at Nahal Raqefet and Muhraqa) yielded a whole-rock age of 96.7 ± 0.5 Ma. The youngest Cenomanian volcanic intercalation in the Umm el Fahm area (basalt at Me-Ammi) yielded a whole-rock age of 95.4 ± 0.5 Ma. Amphiboles from the Senonian Bat Shelomo pyroclastics, the youngest volcanic unit in the area, yielded an age of 82.0 ± 1.3 Ma.

Three conclusions may be drawn from our new radiometric ages: (1) The major volcanic events operated synchronously at Mount Carmel and the Umm el Fahm area. (2) The chalk complex of Mount Carmel and the Deir Hanna Formation in the Umm el Fahm area are stratigraphically correlated. (3) The new radiometric results agree with biostratigraphically-derived ages, but provide better time constraints for the lithostratigraphic units. The data help to settle previous correlation controversies: the Albian–Cenomanian boundary is set below the top of the Yagur Formation, and the Cenomanian–Turonian boundary, above the base of the Muhraqa Formation.

INTRODUCTION

Mount Carmel and the Umm el Fahm area are the only localities in northern Israel where Late Cretaceous volcanic activity is recorded (Sass, 1968, 1980; Sass and Bein, 1982; Garfunkel, 1989). Basaltic volcanic units, predominantly pyroclastics at Mt. Carmel and mostly flows in the Umm el Fahm area, are interbedded within a ~300-m-thick sequence of marine carbonates. These units have great potential for use in stratigraphic correlation. Conventional stratigraphic correlation has been difficult in this area for three reasons:

E-mail: amit.segev@mail.gsi.gov.il

 0021-2164/02 $4.00

1. Facies changes are common in the Mount Carmel sequence, related to the proximity of the area to the platform edge during the Cenomanian and Turonian, and to the effect of protruding structures (reefs, volcanoes) on adjacent and distal environments. In contrast, the Umm el Fahm area was located at the inner part of the platform and is characterized by monotonous and gradual facies variations.
2. The Mount Carmel sequence is intensively faulted (Picard and Kashai, 1958; Ron et al., 1990), making it difficult to track facies changes across fault blocks.
3. Mount Carmel is separated from the adjacent Umm el Fahm area by a syncline (Fig. 1), that does not allow direct comparison of stratigraphic boundaries across the different platform subenvironments (edge, inner part).

Stratigraphic correlation using the volcanic units has been only partly successful due to their limited geographic extent. While correlation is theoretically feasible for distances up to ~10 km, it is impractical for larger distances, such as between the northern and southern parts of Mount Carmel, or between Mount Carmel and the Umm el Fahm area. Using the absolute ages of the volcanic rocks and imposing the constraints of geomagnetic polarity data, we hoped that correlation would be possible over a larger area.

This paper presents a preliminary chronostratigraphic framework for the Upper Cretaceous section in Mount Carmel and the Umm el Fahm area, integrating new $^{40}Ar/^{39}Ar$ age determinations and paleomagnetic analyses with published biostratigraphic data.

GEOLOGICAL SETTING

Mount Carmel (MC) and the Umm el Fahm area (UFA) are elevated topographic features separated by a syncline (Fig. 1). Both consist of Cretaceous marine successions, subdivided into two parts (Fig. 2), the older Judea Group (hard carbonate rocks) and the overlying Mount Scopus Group (mostly soft carbonates and marls). The Mount Scopus Group is quite uniform across a wide area in northern Israel, but Judea Group sections at both localities are quite dissimilar.

Stratigraphic relationships within the Judea Group of Mount Carmel (Fig. 2) are quite complicated, as marked facies changes occur across short and long distances (Kashai, 1958; Picard and Kashai, 1958; Bein, 1974, 1977; Sass, 1980; Sass and Bein, 1982). Central and northern Carmel are made up principally of the "Main Chalk Complex" (Picard and Kashai, 1958), which overlies the dolomitic Yagur Formation. In contrast, in the southern part, the equivalent section consists mostly of limestones, dolomites, and reef structures. Lithostratigraphic correlation between the northern and southern areas is uncertain and controversial. The Main Chalk Complex is overlain by a succession of reef-related limestones (reef cores, reef talus, bioclastic limestones), dolomite in places, and an intermediate marl unit (comprising the Muhraqa, Daliyya, and Umm E Zinat formations). Southward, the marl unit wedges out and disappears, reef structures are scarce, and an undivided limestone succession (the Shune Formation) is found. Locally developed volcanic rock units, mostly pyroclastic, are common as lenticular intercalations in the chalk and in the equivalent limestone/dolomite succession. Each of these units has a limited lateral extent (up to ~6 km) and a maximum thickness of ~60 m.

Stratigraphic relationships in the Umm el Fahm area are much simpler, and the major lithostratigraphic units retain their identity over the entire area (Fig. 2). The Cretaceous section, roughly equivalent to that at MC, consists of the Deir Hanna and Sakhnin formations, dolomitic divisions that display no evident similarity or correlation with MC. The only similarity is the occurrence of volcanic intercalations in both areas, but there are significant differences between the two areas. The volcanic intercalations in the UFA are restricted to the Deir Hanna Formation. Most of the volcanic units at MC occur in the Cenomanian chalk and equivalent limestone/dolomite sections, while a single one is contained in the younger Senonian En Zetim Formation. Most of the volcanic rocks in the UFA are basaltic lava flows, with the exception of the youngest unit, which consists of pyroclastics. The opposite is true at MC, where most of the volcanic units are pyroclastics, and basaltic lava flows terminate the local volcanic activity. Of the five volcanic units in the UFA, only the two lower ones have a restricted extent. The other units persist across the entire areas of their exposed host stratigraphic units, with variations in thickness.

In summary, the Judea Group sections at MC and the UFA are quite dissimilar. This observation, combined with the scarcity of index fossils in dolomites and in most limestones, has produced controversy in stratigraphic correlations (Fig. 2). According to some authors (e.g., Bartov et al., 1981; Flexer et al., 1981), the Chalk Complex at MC correlates with both the Deir Hanna and Sakhnin formations of the UFA, and

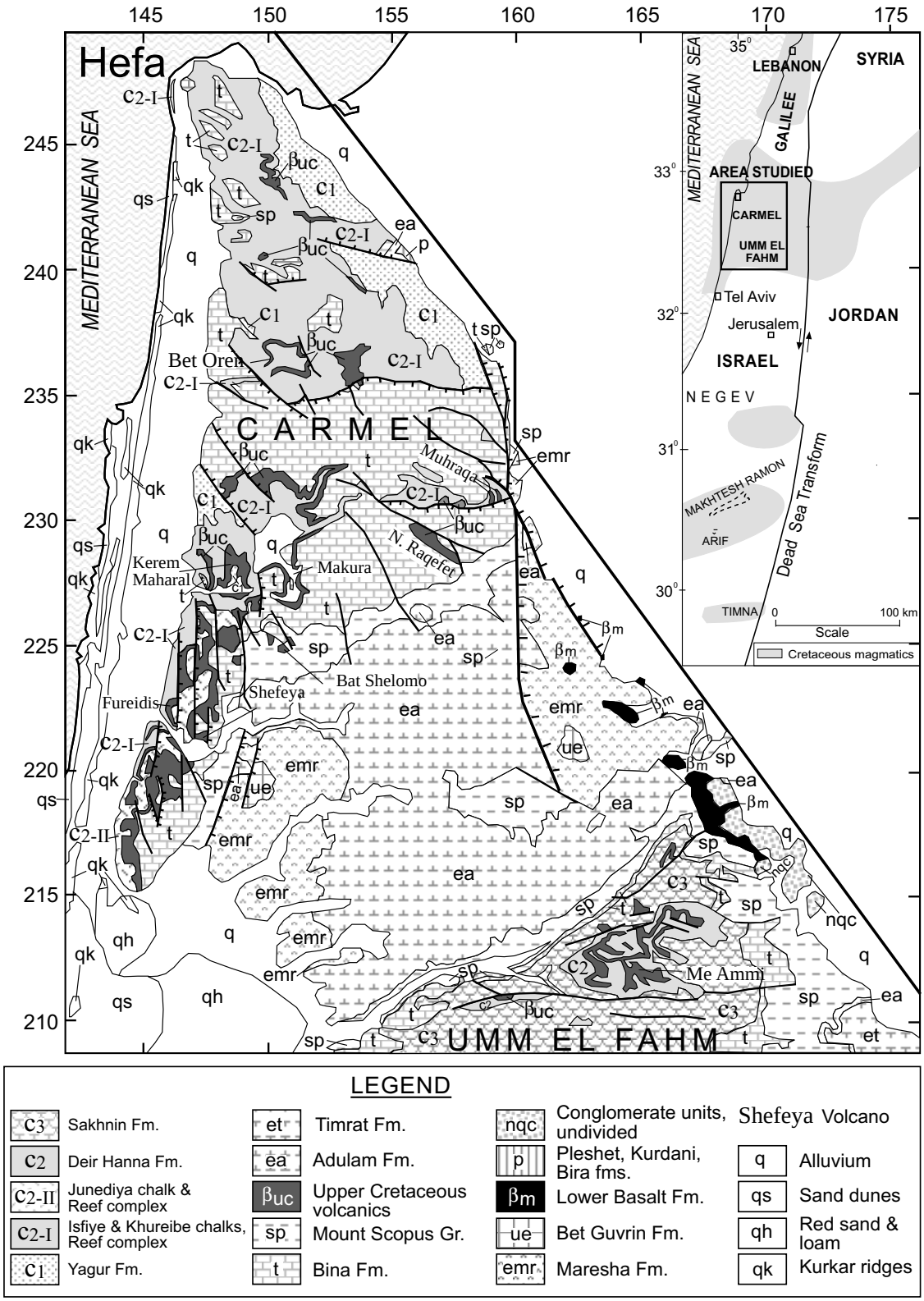

Fig. 1. Geological map of Mount Carmel and the Umm el Fahm area. Coordinates, old Israel Grid.

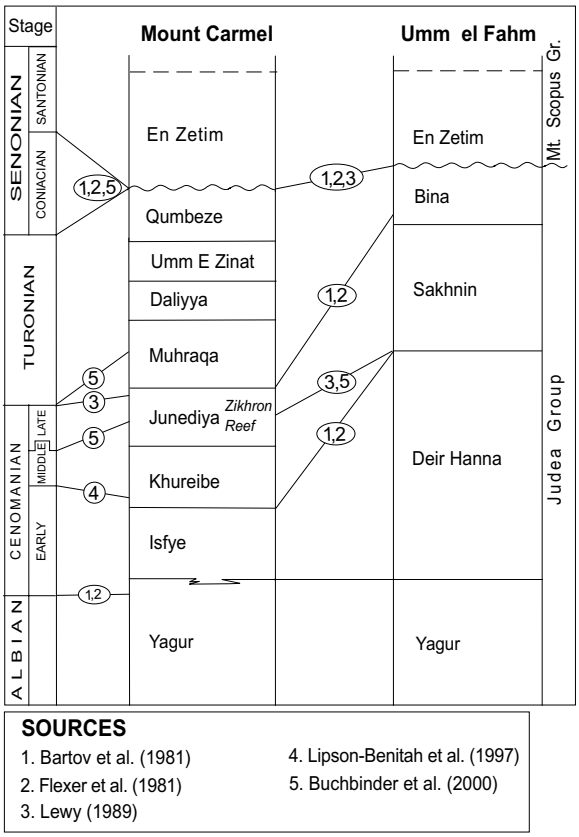

Fig. 2. Lithostratigraphic relationships of the Judea Group in Mt. Carmel and the Umm el Fahm area.

the Muhraqa–Daliyya–Umm E Zinat formations (or equivalent Shune Formations), together with the overlying Qumbeze Formations, are equivalent to the Bina Formations. Others (Lewy, 1989; Buchbinder et al., 2000) correlate the Chalk Complex of MC with the Deir Hanna Formations, and the Muhraqa–Daliyya–Umm E Zinat–Qumbeze formations with the Sakhnin–Bina Formation.

SAMPLING AND GEOCHRONOLOGY

Mount Carmel

Kerem Maharal volcano (coord. 1487/2283)

Outcrops of black to variegated pyroclastics occur in isolated areas west of Kerem Maharal. This rock unit overlies the Yagur Formation and represents the first volcanic eruption in the area. The pyroclastics contain xenoliths of garnet, clinopyroxenite and rare peridotite, and olivine gabbro. Xenocrysts of augite, garnet, hornblende, biotite, and spinel are very common and appear to have resulted from xenolith disintegration (Sass, 1980). Hornblende crystals (AS-9811, 9812) and a basaltic bomb (AS-9816) were collected at this site.

Raqefet (coord. 1560/2295) and the Muhraqa (coord. 1589/2311) lavas

The Raqefet volcanic complex includes three volcanic units, two lower pyroclastic units and an upper ~25 m section of olivine basalt flows (Sass, 1980). The nearby Muhraqa lavas (~4 km east of Nahal Raqefet) consist of porphyritic olivine basalt and appear to be correlated with the Raqefet lava flows. Fresh samples of both lavas were sampled (S_{2-3} from Nahal Raqefet and S_{2-4} from Muhraqa, Table 1).

Table 1
Samples used for $^{40}Ar/^{39}Ar$ age determinations

Sample	Location	Coord. (Old Israel Grid)	Igneous Unit	Type of sample	K (%)	Lab
Mount Carmel						
AS-9816	Kerem Maharal	1487/2283	Tuff near vent	WR basaltic bomb	0.25	1
AS-9811	Kerem Maharal	1487/2283	Tuff near vent	Amphibole sing. crys.	1.8	1
S_{2-3}	Nahal Raqefet	1560/2295	Upper basalt flow	WR		2
S_{2-4}	Muhraqa	1589/2311	Upper basalt flow	WR		2
AS-99/3	Bat Shelomo	1509/2250	Volcaniclastics near vent	Amphibole sing. crys.	1.61	1
Umm el Fahm						
S_{2-2}	Me-Ammi	1634/2121	Upper basalt flow	WR		2
AS-99/1A	Me-Ammi	1634/2121	Upper basalt flow	Plagioclase separate #	0.55	1
AS-99/1B	Me-Ammi	1634/2121	Upper basalt flow	Plagioclase separate #	0.99	1

sing. crys.—single crystal; WR—whole rock; #—XRD-identified.
1—Geological Survey of Israel; 2—Stanford University.

Bat Shelomo volcano (coord. 1509/2250)

The small Bat Shelomo volcanic vent is located in a chalk host section of Senonian age and terminates the Cretaceous magmatic activity. It consists of ~30 m of dark pyroclastic rocks containing ejecta of sedimentary blocks, volcanic bombs, xenoliths, and xenocrysts of hornblende (Sass, 1980). K-Ar ages of three amphibole single crystals from Bat Shelomo average 82 ± 2 Ma (Segev, 2000, based on unpublished data by Lewy et al.). An amphibole crystal from this vent was collected and dated in this study (AS-99/3) (Table 1).

Umm el Fahm area

Me-Ammi upper lava flow (coord. 1641/2118)

The Me-Ammi basalt flow and the overlying pyroclastic rocks (DHv_4 and DHv_5, respectively; Sass, 1968), in the upper Deir Hanna Formation, terminate the volcanic activity in the UFA. One whole-rock sample from the Me-Ammi lava flow was collected and dated at Stanford University ($S_{2\text{-}2}$), and two aliquots of plagioclase from a second sample were dated at the Geological Survey of Israel, GSI (AS-99/1A and 1B, Tables 1, 2).

METHODS

Samples analyzed at the GSI laboratory were first crushed and sieved. The 120–170 mesh (0.105–0.088 mm) fraction was divided using a Franz magnetic separator. A low susceptibility fraction containing principally plagioclase was separated from a higher susceptibility fraction containing olivine, pyroxene, and amphibole. The matrix separates contain disseminated magnetite and, thus, were found mainly in the high susceptibility fractions. The A and B fractions of sample AS-99/1 are clean non-magnetic minerals containing only very minor matrix (probably pyroxene, see the Fe and Ca content in Table 2).

The $^{40}Ar/^{39}Ar$ measurements at the GSI were conducted using procedures as described in Heimann et al. (1992). Samples were irradiated in the IRR-1 reactor at the Soreq Nuclear Center, Israel (Heimann et al., 1992). The samples were heated using an inductive furnace and analyzed using an MM-1200B mass spectrometer at the GSI geochronological laboratory. Neutron fluence was calibrated using LP-6 biotite standard with an assumed age of 128.5 Ma (Roddick, 1983).

For conventional K–Ar measurements, potassium was determined after fusing with $Li_2B_2O_4$ by ICP-AES (Perkin Elmer Optima 3000). Argon isotopic measurements were done at the GSI geochronological laboratory using standard isotope dilution and an MM-1200B mass spectrometer (Steinitz et al., 1982).

Plateau ages were calculated using the standard criteria. A plateau is defined by three or more contiguous steps whose apparent ages are not significantly different at 2σ and which contain at least 50% of the released ^{39}Ar (McDougall and Harrison, 1999).

Normal ($^{40}Ar/^{36}Ar$ vs. $^{39}Ar/^{36}Ar$) and inverse ($^{36}Ar/^{40}Ar$ vs. $^{39}Ar/^{40}Ar$) isotope correlation diagrams were generated using Isoplot 2.3 (Ludwig, 2000). Normal isochrons constructed by a Model 1 fit are based on the York (1969) algorithm. On the assumption that the assigned uncertainties are the only reason the data diverge from a straight line, the points are weighted proportionally to the inverse square of their uncertainty (allowing for correlated uncertainties). The Mean Square of Weighted Deviates (MSWD) expresses the goodness of fit, using these assumptions. The uncertainties are quoted at the 2σ level assigning a 1.5% error to J. If the assigned uncertainties are the only cause of scatter, the MSWD tends towards 1, while MSWD values much greater than 1 suggest either underestimated analytical errors, or the presence of non-analytical scatter (Ludwig, 2000).

The plateau and isochron ages for all the samples are generally concordant. We use only isochron ages for comparison, as they are not influenced by the choice of the $^{40}Ar/^{36}Ar$ ratio of the trapped non-radiogenic ^{40}Ar. For samples measured at GSI, the normal isochrons were used for age interpretation.

Three $^{40}Ar/^{39}Ar$ analyses of WR basalt samples

Table 2
Chemical analyses (major constituents) of the studied samples (results in wt %)

Sample	SiO_2	Al_2O_3	Fe_2O_3	TiO_2	CaO	MgO	MnO	Na_2O	K_2O	P_2O_5	SO_3	L.O.I.	Total
AS-9816 WR	40.0	8.0	14.5	3.30	9.40	12.70	0.21	0.60	0.30	0.10	0.05	4.32	93.5
AS-9816	43.5	8.0	10.0	1.70	9.80	14.50	0.10	0.60	0.50	0.05	0.05	4.37	93.2
AS-99/1 WR	47.0	12.5	13.0	2.80	8.80	10.20	0.15	2.50	1.15	0.05	0.05	0.45	98.6
AS-99/1B	54.5	25.0	1.9	0.25	8.90	1.60	0.02	4.70	1.20	0.05	0.05	0.76	99.0
AS-99/1A PL	55.5	27.1	1.1	0.15	10.60	0.70	0.05	4.85	0.67	0.10	0.10	0.36	101.3

(S_{2-2}, S_{2-3}, and S_{2-4}) were done at Stanford University. These samples were irradiated at the USGS TRIGA reactor; the argon was extracted in a vacuum furnace and analyzed with a MAP 216 mass spectrometer (Hacker et al., 1993). Neutron fluence estimates used Taylor Creek sanidine (85G003 with an assumed age of 27.92 Ma, Izett et al., 1991). For these samples, the inverse isochrons were used for age interpretation.

RESULTS

The chemical composition of most of the fractions used for $^{40}Ar/^{39}Ar$ measurements at GSI was determined, and the purity of the mineral separates was checked by XRD (Tables 1 and 2). K/Ar ages of amphibole megacrysts from Kerem Maharal are listed in Table 3. The $^{40}Ar/^{39}Ar$ data are illustrated in Figs. 3–5, and a summary of all the age determinations is presented in Table 4.

Table 3
K/Ar data of two amphibole crystals from the Kerem Maharal volcano, Mount Carmel

Sample	$^{40}Ar_{rad}$ (ppb wt.)	$^{40}Ar_{rad}$ (%)	K (% wt)	Age (Ma)
AS-9821	7.18	95.9	1.80	100.0 ± 2.8
AS-9821	7.17	96.3	1.80	99.9 ± 2.0

[a]Decay and isotopic constants as suggested by Steiger and Jäger (1977).

All apparent age spectra for WR samples show a disturbance at low and high temperatures but display well-defined plateaus in the intermediate temperature steps. The amphibole apparent age spectra are flat with varying degrees of disturbance at both ends, and the plagioclase separates yield relatively flat spectra.

Kerem Maharal volcano

An amphibole megacryst (AS-9811) from this volcano yielded a somewhat disturbed plateau age of 96.9 ± 0.7 Ma (Fig. 3a), defined by 97% of cumulative released ^{39}Ar (8 contiguous steps; Table 4). Five of six low temperature steps (3% of cumulative released ^{39}Ar) yielded older apparent ages (up to 120 Ma) and suggest the presence of excess ^{40}Ar. The isochron age (97.1 ± 1.7 Ma, MSWD = 0.4 with $^{40}Ar/^{36}Ar$ of 301 ± 20; Fig. 3b) is concordant with the plateau age. The K/Ar age of another amphibole crystal is slightly older (99.9 ± 2.0 Ma, Table 3), but is not significantly different from the isochron age.

The WR basaltic bomb (AS-9816) from the same site yielded a disorderly, and probably meaningless, apparent age spectrum (Fig. 3c), and a total gas date of 111 ± 56 Ma with no statistically valid isochron.

Nahal Raqefet volcano

The WR sample from Nahal Raqefet upper basaltic flow (S_{2-3}) yielded a plateau age of 96.5 ± 0.1 Ma (Fig. 4a), defined by 84% of cumulative released ^{39}Ar (7 contiguous steps; Table 4). Its concordant inverse isochron age is 96.9 ± 0.2 Ma with MSWD = 0.86 and

Table 4
Summary of $^{40}Ar/^{39}Ar$ age calculations for whole rock and mineral separates

Sample	Lab	Sample type	Total gas age (Ma)	Plateau data				Isochron calculations				
				Step nos.	^{39}Ar (%)	Age (Ma)	Error (Ma)	Type	Age (Ma)	Error (Ma)	40/36 Intercept	MSWD
Mount Carmel												
AS-9811	GSI	amph*	97 ± 1.5	7–14	97	96.9	0.7	N	97.1	1.7	301 ± 20	0.35
AS-9816 WR	GSI	WR	111 ± 56	—	—	—						
S_{2-3}	Stan	WR	94 ± 1.5	4–10	84	96.5	0.1	I	96.9	0.2	283 ± 5	0.86
S_{2-4}	Stan	WR	76 ± 17	3–9	88	96.0	0.4	I	96.5	0.5	288 ± 8	0.07
AS-99/3	GSI	amph*	81 ± 1	2–7	95	81.1	0.6	N	82.0	1.3	296 ± 110	0.08
Umm el Fahm												
S_{2-2}	Stan	WR	91 ± 5	5–11	72	95.3	0.3	I	95.4	0.5	285 ± 9	0.43
AS-99/1A	GSI	plag	93 ± 2	6–11	73	93.6	0.9	N	95.5	3.7	270 ± 57	0.52
AS-99/1B	GSI	plag	96 ± 1.5	6–15	52	95.1	0.7	N	97.5	4.9	214 ± 210	0.1

GSI—Geological Survey of Israel; Stan.—Measurements at Stanford University; amph*—Different amphibole single crystal; N—Normal isochron; I—Inverse isochron.

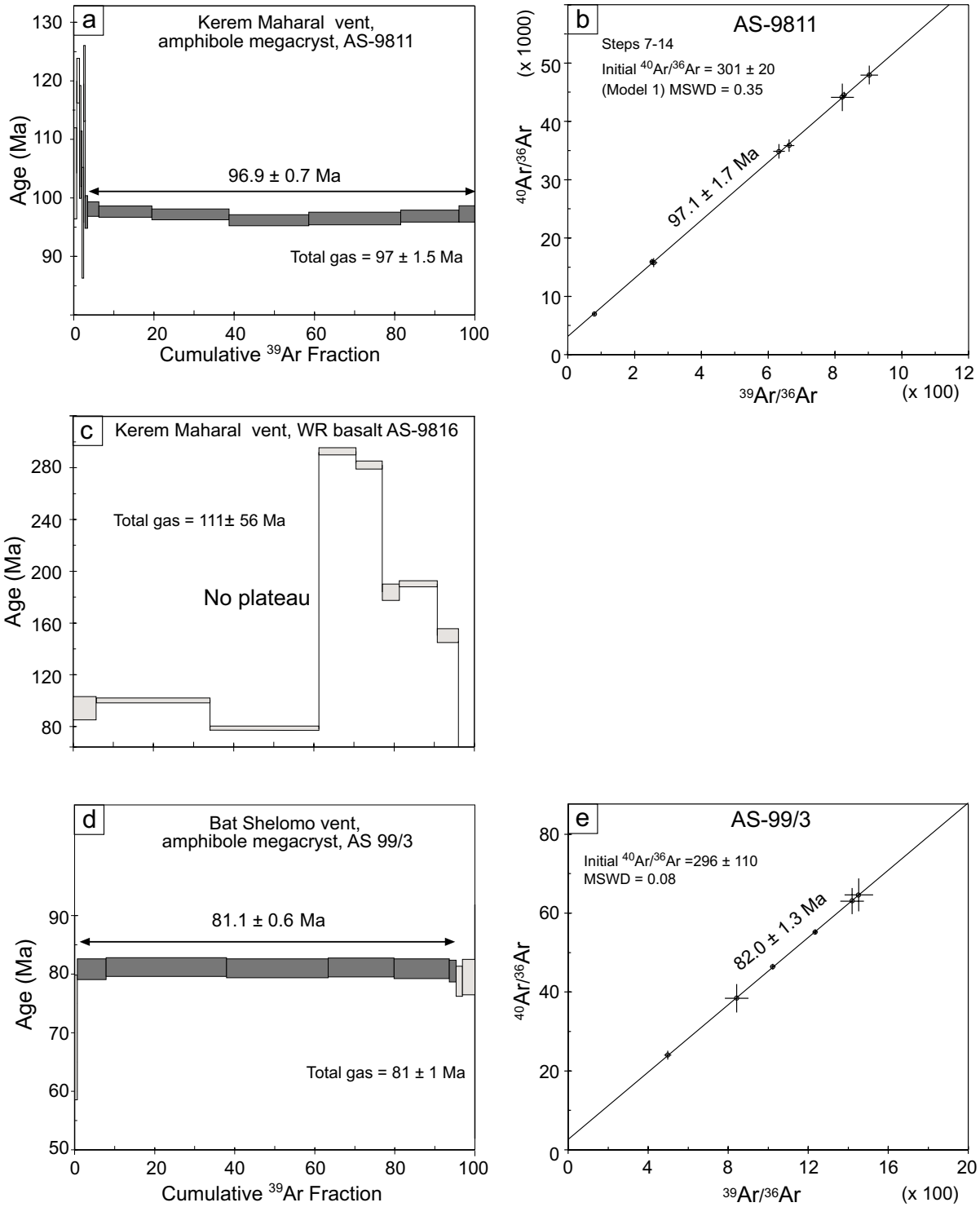

Fig. 3. ^{40}Ar-^{39}Ar age spectra and normal isochron ages for Kerem Maharal and Bat Shelomo volcanoes, Mount Carmel.

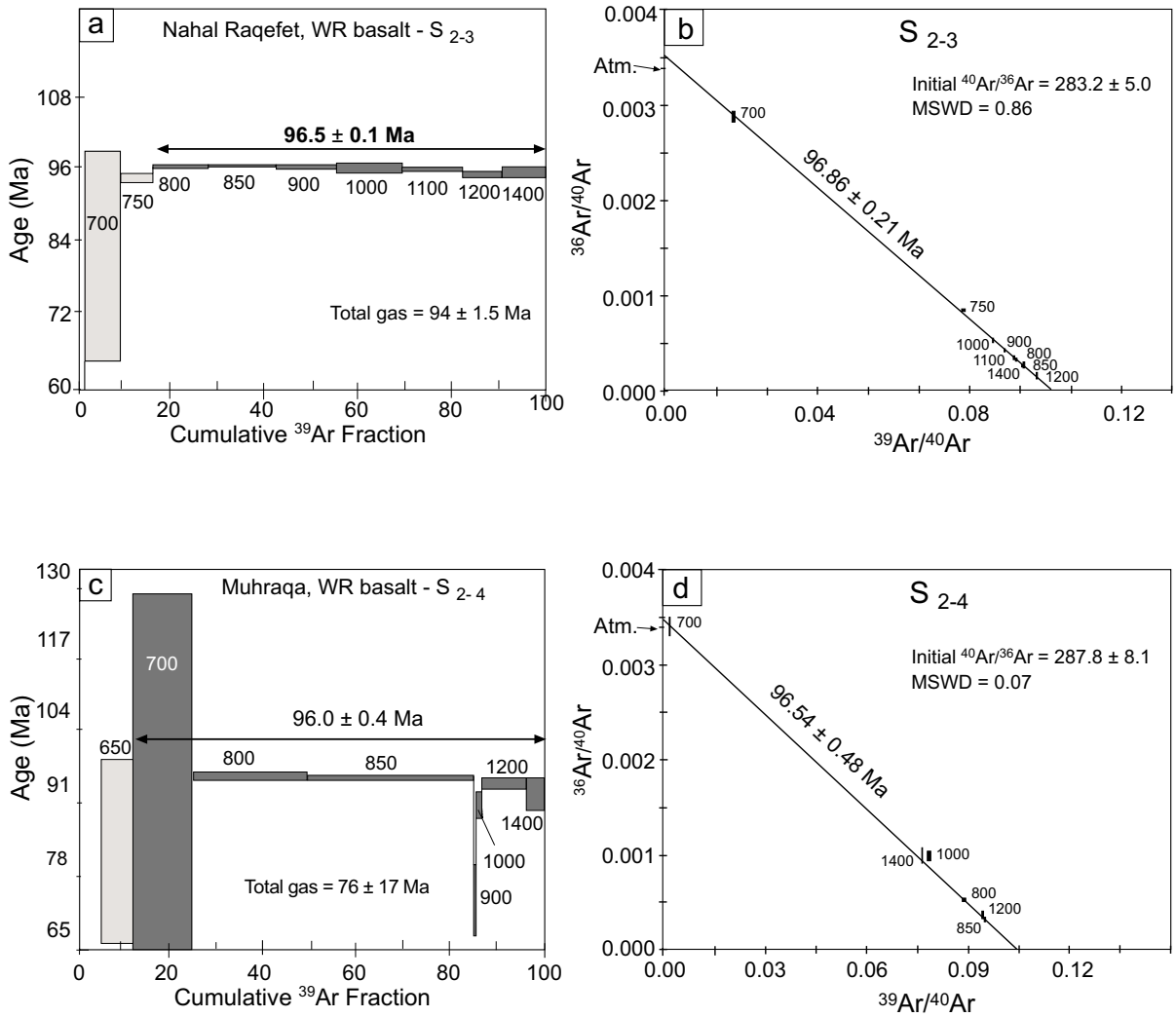

Fig. 4. ^{40}Ar-^{39}Ar age spectra and inverse isochron ages for Nahal Raqefet and Muhraqa upper lava flows, Mount Carmel. Step temperature recording included by the standard analytical procedure at the Stanford laboratory.

a $^{40}Ar/^{36}Ar$ intercept of 283 ± 5 (Fig. 4b). Similarly, the WR sample from the correlative Muhraqa upper basaltic flow (S_{2-4}) yielded a plateau age of 96.0 ± 0.4 Ma (Fig. 4c), defined by 88% of the cumulative released ^{39}Ar (7 contiguous steps; Table 4). The concordant inverse isochron age is 96.5 ± 0.5 Ma, with MSWD = 0.1 and a $^{40}Ar/^{36}Ar$ intercept of 288 ± 8 (Fig. 4d). These two basalts represent a single volcanic event.

Bat Shelomo Volcano

One amphibole megacryst (AS-99/3) from this volcano was dated by both the Ar/Ar and K/Ar methods. Two amphibole megacrysts were previously dated by K/Ar in duplicate (BL-1001 and BL-1002; Segev, 2000, based on unpublished data by Lewy et al.). The amphibole AS-99/3 yielded a well-defined plateau with an age of 81.1 ± 0.6 Ma (Fig. 3d), defined by 95% of the cumulative released ^{39}Ar (6 contiguous steps; Table 4), similar to its total gas age of 81 ± 1 Ma and concordant with the isochron age of 82.0 ± 1.3 Ma (MSWD = 0.1; Fig. 3e), with initial $^{40}Ar/^{36}Ar$ ratio of 296 ± 110. The weighted average of five K/Ar ages is 82.2 ± 1.8 Ma (data from Segev, 2000), similar to the Ar/Ar ages.

Me-Ammi upper basaltic flow

The WR sample from Me-Ammi upper basaltic flow (S_{2-2}) yielded a plateau age of 95.3 ± 0.3 Ma (Fig. 5a)

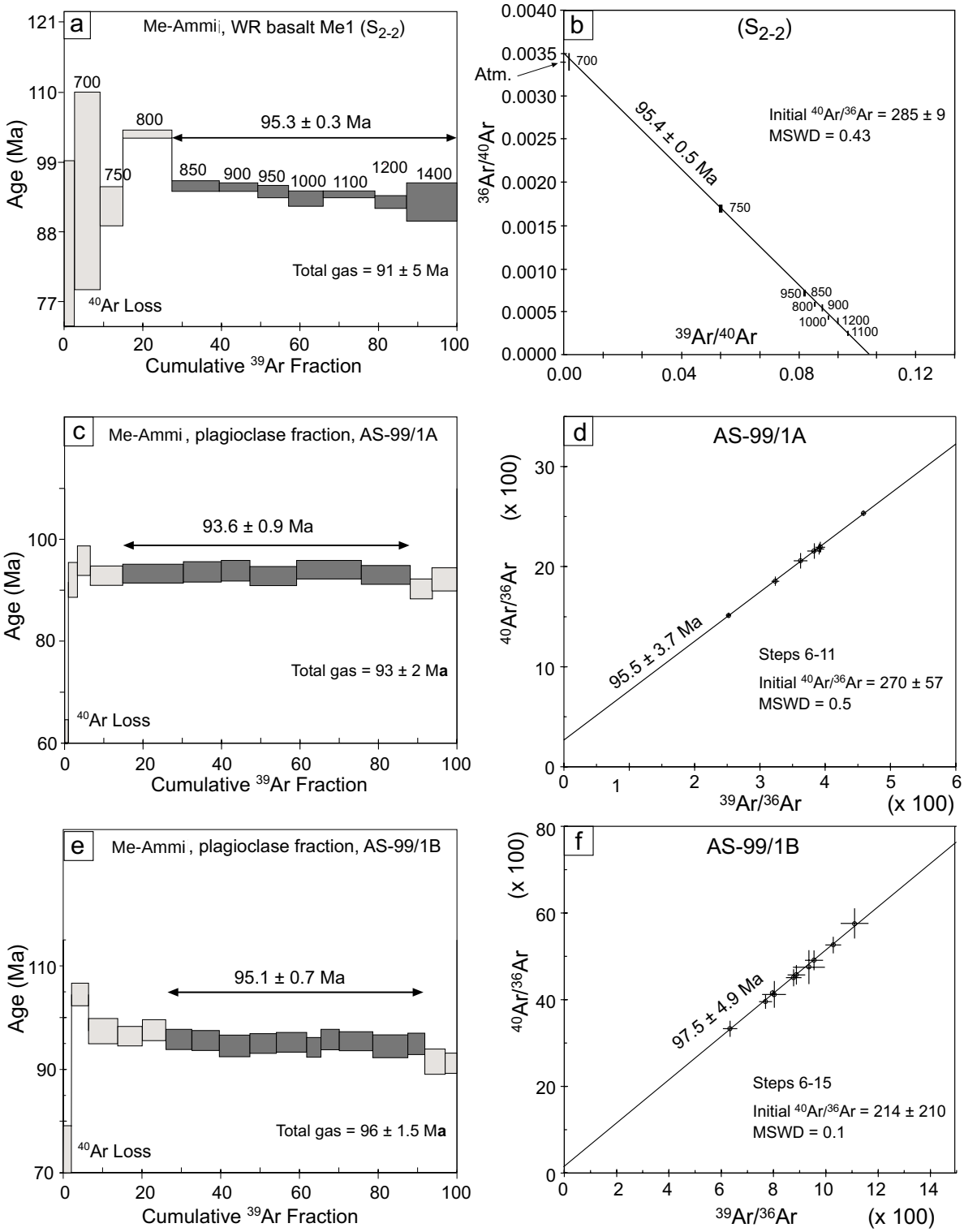

Fig. 5. ^{40}Ar-^{39}Ar age spectra and isochron ages for Me-Ammi lava flow, Umm el Fahm area. WR = a and b step temperature recording included by the standard analytical procedure at the Stanford laboratory. Plagioclase separates = c, d and e, f.

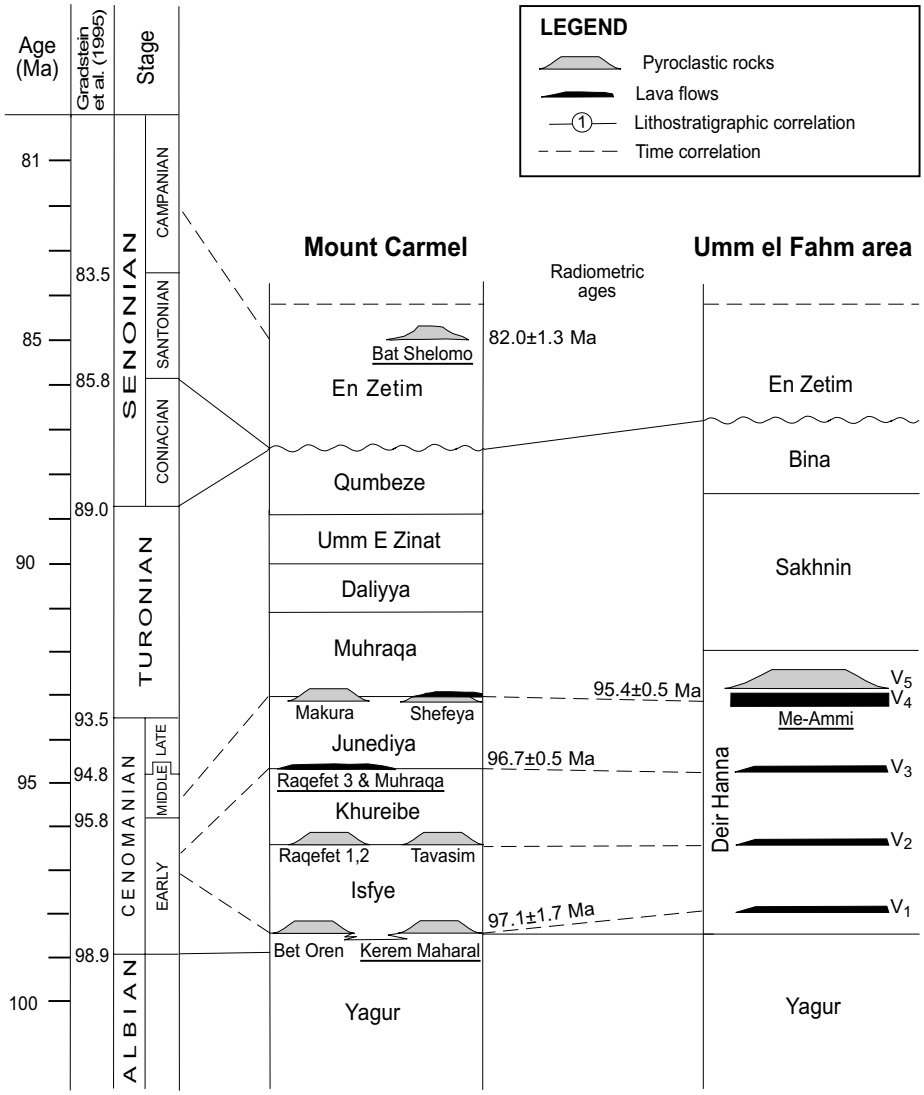

Fig. 6. Chrono- and litho-stratigraphic correlation in Mount Carmel and the Umm el Fahm area. The given radiometric ages refer to the respective underlined volcanic sites.

defined by 72% of cumulative released ^{39}Ar (7 contiguous steps; Table 4). Its concordant inverse isochron age is 95.4 ± 0.5 Ma with MSWD = 0.4 and an $^{40}Ar/^{36}Ar$ intercept of 285 ± 9 (Fig. 5b).

Two plagioclase concentrates (AS-99/1A and AS-99/1B) from the same basaltic flow yielded well-defined plateau ages of 93.6 ± 0.9 and 95.1 ± 0.7 Ma (Fig. 5c,e, respectively). Both plagioclase fractions yielded concordant isochron ages of 95.5 ± 3.7 and 97.5 ± 4.9 Ma, with MSWD = 0.5 and 0.1, respectively (Fig. 5d,f). The $^{40}Ar/^{36}Ar$ intercepts of these isochrons are 270 ± 57 and 214 ± 210.

PALEOMAGNETISM

Methods and results

New paleomagnetic data were obtained from the same Cenomanian samples that we used for our age determinations. Samples from Muhraqa, Nahal Raqefet, and Me-Ammi (Ron et al., 1990) were collected as field-drilled cores and oriented by sun compass. Senonian volcanic pyroclastic samples from Bat Shelomo were also collected and oriented in the field in 2 × 2 × 2-cm plastic boxes. Natural remanent magnetization (NRM) was measured and stepwise demagnetized in a three-

axis cryogenic magnetometer with integrated alternating field (AF) coils. All samples retained 90% of their NRM after demagnetization to 80 mT and display stable magnetic behavior. Most of the samples display single component vectors, but some display two-component behavior with a low coercivity viscous remanent magnetization (VRM) component of recent origin superimposed on a stable characteristic remanent magnetization (ChRM). The demagnetization behavior of all samples is suggestive of titanomagnetite as the carrier of remanence. All samples yield ChRM with shallow inclination and N to NNE declination (Fig. 7).

A compilation of all paleomagnetic data is presented in Table 5. The detailed analytical procedures and statistics can be found in Ron et al. (1990).

All Cenomanian samples display positive shallow inclinations, as expected for stable Africa (Table 5). The divergent NNE declinations result from vertical axis rotation of fault blocks bounded by strike slip faults (Ron et al., 1990). From the mean inclination, we estimate the paleolatitude of the region during Cenomanian time to be ~7°N. The paleolatitude estimated from the Senonian rocks is ~14°N, but this estimate cannot be considered reliable because directions from only a single site are available.

DISCUSSION

The radiometric ages

Amphibole from Kerem Maharal yielded a plateau age of 96.9 ± 0.7 Ma with a concordant isochron age of 97.1 ± 1.7 Ma. As discussed previously, we take the isochron age of the amphibole as representative of the cooling age, and hence the eruption time of the Kerem Maharal volcano. The small amount of excess ^{40}Ar

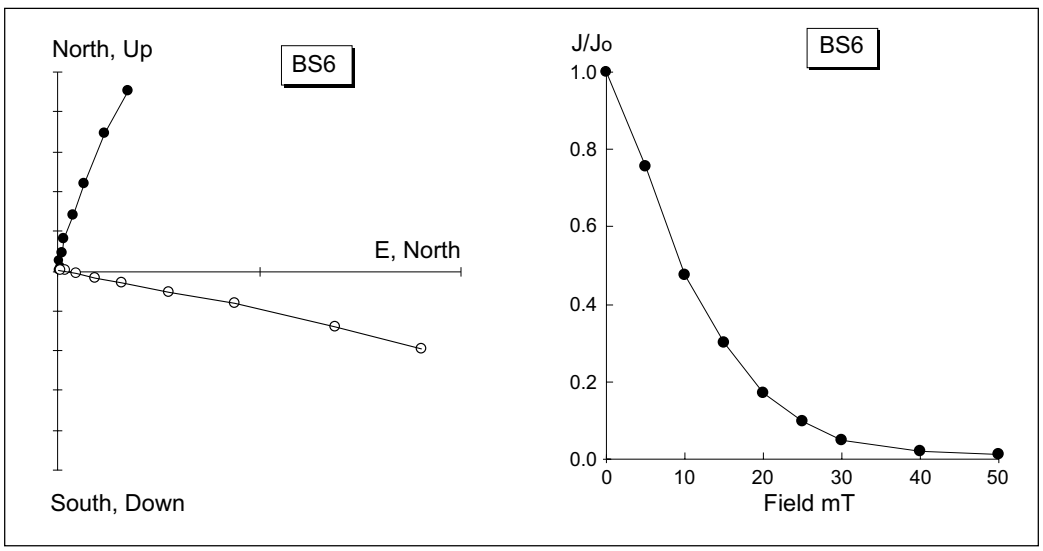

Fig. 7. Orthogonal magnetic vector plot and normalized intensity (J/J_0) of a representative sample of normal polarity from Bat Shelomo volcano showing stepwise demagnetization in an alternating field (AF). Solid circles denote the declination component and open circles denote the inclination component.

Table 5
Compilation of observed (O) and expected (E) paleomagnetic field directions of Mount Carmel region. The VGP data for the stable African Plate are from Besse and Courtillot (1991)

Age	Dec. (O)	Inc. (O)	α 95	n	VGP (Ma)	λ (N)	Φ (E)	Dec. (E)	Inc. (E)
Cenomanian	9.4	13.5	6.3	14	98.4	61.6	245.6	345.9	14.7
Senonian	7.8	26.7	8.2	6*	80.7	66.4	232.2	353.1	19.3

n—number of sites, and with *, number of samples; Dec.—Declination; Inc.—Inclination; α 95—radios of 95% confidence about the mean; VGP (Ma)—age of the Virtual Geomagnetic Pole of the stable African Plate; λ (N)—VGP latitude; Φ (E)—VGP longitude.

may result from contamination by older basement during uprising of the magma (e.g., Renne, 1995) and explains the slightly older (~3 m.y.) K/Ar apparent age. The WR bomb sample from the same site yielded a meaningless date, possibly caused by alteration.

The whole-rock basalt samples from Nahal Raqefet and Muhraqa yielded isochron ages of 96.9 ± 0.2 and 96.5 ± 0.5 Ma, respectively. Since these samples belong to the same unit (the upper basalt flows in the western Carmel area), their average isochron age of 96.7 ± 0.5 Ma is probably its crystallization age.

The terminal Late Cretaceous (Senonian) volcanic eruption in the Carmel area (Bat Shelomo volcano) is well dated by amphibole, whose flat and undisturbed spectrum yielded an age of 81.1 ± 0.6 Ma. The companion isochron age is 82.0 ± 1.3 Ma. This age dates the cooling of the amphibole and, in turn, the eruption age of the Bat Shelomo volcano. The isochron age is in agreement with the average K–Ar age calculated from five single-crystal measurements (82.2 ± 1.8, data from Segev, 2000).

The Me-Ammi lava flow in the Umm El Fahm area was dated at two laboratories. A whole-rock sample was analyzed at Stanford, and yielded a plateau age of 95.3 ± 0.3 Ma and a concordant inverse isochron age of 95.4 ± 0.5 Ma. The two low-susceptibility fractions from the same basaltic flow consist mainly of plagioclase, and were dated at GSI, yielding plateau ages of 93.6 ± 0.9 and 95.1 ± 0.7 Ma, with 95.5 ± 2.2 and 97.5 ± 4.9 Ma isochron ages. The whole-rock sample yielded a much smaller analytical error, and therefore we take 95.4 ± 0.5 Ma to be the cooling age of the Umm el Fahm upper lava flow.

Paleomagnetic evidence

The paleolatitude from our measurements at Bat Shelomo volcano is ~14°N, whereas the expected value derived from stable Africa is 10°N (Besse and Courtillot, 1991). This 4° difference is probably due to insufficient averaging of secular variation. Both are consistent with northward drift of Africa at the end of the Cretaceous. Our data further confirm the assumption that the Sinai–Israel sub-plate was part of stable Africa during the Mesozoic. The positive inclination and northerly declination at this site may indicate that these volcanics were magnetized near the end of the Chron 34 normal polarity interval. The age of the Senonian Bat Shelomo pyroclastic rocks is 82.0 ± 1.3 Ma, slightly younger than the 34n/33r polarity boundary (83.0 Ma, after Cande and Kent, 1995), but the age difference is not statistically significant.

Radiometric ages and stratigraphic correlation

Our new ages provide constraints for existing correlation schemes and help define the tentative stratigraphic correlation presented in Fig. 6. The volcanic units we dated in the Judea Group in both areas are Cenomanian in age. Our first assumption is that the undated volcanic units (the upper equivalent units Shefeya and Makura in MC, as well as the three lower units in the UFA) are also included in this time interval. Next, four main volcanic episodes are present at both MC and the UFA. Formally, five units have been recognized in the UFA (Sass, 1968), but upper units V_4 and V_5 can be considered as substages of one episode since they are separated in places by a thin limestone layer that is absent elsewhere. In view of the relatively short distance between the two areas, we think that each of the major volcanic episodes was synchronous over the entire area. Accordingly, we propose a correlation of the main Cenomanian volcanic units in MC with corresponding units in the UFA (Fig. 6).

This correlation is not totally consistent with the preliminary correlation of volcanic bodies in Mount Carmel of Sass (1980), and in particular with the view that the lavas of Shefeya, Raqefet 3, and Muhraqa are time equivalents. The previous correlation was based on the observation that there is only one basalt unit in each of the three mentioned areas, which represents the terminal volcanic activity in this area. It had been assumed that these three basalts are local manifestations of one episode, but our new radiometric data point to a gap of 1.3 m.y. between the youngest basalt in the UFA and the Raqefet 3-Muhraka basalts in MC, which is larger than the analytical uncertainty.

This proposed correlation scheme has two important chronostratigraphic implications. First, the Chalk Complex at Mount Carmel can be correlated with the Deir Hanna Formation in the Umm el Fahm area. Second, setting the Albian–Cenomanian boundary below the top of the Yagur Formation (Bartov et al., 1981; Flexer et al., 1981; Sass and Bein, 1982) and the Cenomanian–Turonian boundary above the base of the Muhraqa Formation (Buchbinder et al., 2000) is consistent with our ages.

ACKNOWLEDGMENTS

The authors express their thanks to Y. Harlavan for initial data processing and calculations, P. Kotlarsky and C. Dallal for help at the geochronological laboratory, D. Stieber, O. Yoffe, and S. Ehrlich for the potas-

sium analyses, and B. Katz for editing the manuscript. The comments by G. Steinitz and an anonymous reviewer helped us to improve the quality of this paper.

REFERENCES

Bartov, Y., Arkin, Y., Lewy, Z., Mimran, Y. 1981. Regional stratigraphy of Israel: a guide for geological mapping. Geol. Surv. Isr. Stratigraphic Table.

Bein, A. 1974. Reef development in the Judea Group from the coastal plain and the Carmel. Ph.D. thesis, Hebrew Univ., Jerusalem, 193 pp. (in Hebrew, English summary).

Bein, A. 1977. Shelf basin sedimentation: mixing and diagenesis of pelagic and clastic Turonian carbonates, Israel. J. Sediment. Petrol. 47: 382–391.

Besse, J., Courtillot, V. 1991. Revised and synthetic apparent polar wander paths of the African, Eurasian, North America and Indian plates, and true polar wander since 200 Ma. J. Geophys. Res. 96 (3): 4029–4050.

Buchbinder, B., Benjamini, C., Lipson-Benitah, S. 2000. Sequence development of Late Cenomanian-Turonian carbonate ramps, platforms and basins in Israel. Cretaceous Res. 21: 813–843.

Cande, S.C., Kent, D.V. 1995. A new geomagnetic polarity time scale for late Cretaceous and Cenozoic. J. Geophys. Res. 100: 6093–6095.

Flexer, A., Gill, D., Livnat, A., Tamir, N., Toister, A. 1981. Atlas project (Israel subsurface geology information management system), Part A—explanatory notes. Tel Aviv, Oil Exploration (Investments), 43 pp.

Garfunkel, Z. 1989. Tectonic setting of Phanerozoic magmatism in Israel. Isr. J. Earth Sci. 38: 51–74.

Gradstein, F.M., Agterberg, F.P., Ogg, J.G., Hardenbol, J., Veen, P.V., Thierry, J., Huang, Z. 1995. A Triassic, Jurassic and Cretaceous time scale. In: Berggren, W.A., Kent, D.V., Aubry, M.P., Hardenbol, J., eds. Geochronology, time scales and global stratigraphic correlation. Soc. Sediment. Geol. Spec. Publ. 54: 95–126.

Hacker, B.R., Ernst, W.G., McWilliams, M.O. 1993. Genesis and evolution of a Permian-Jurassic magmatic arc and accretionary wedge, and reevaluation of the terrain concept in the Klamath Mountains. Tectonics 12: 387–409.

Heimann, A., Steinitz, G., Zafrir, H. 1992. Irradiation of samples for $^{40}Ar/^{39}Ar$ dating using the Soreq Nuclear Research Center IRR-1 reactor, Israel. Nucl. Geophys. 6: 273–286.

Izett, G.A., Dalrymple, G.B., Snee, L.W. 1991. $^{40}Ar/^{39}Ar$ age of Cretaceous-Tertiary boundary tektites from Haiti. Science 252: 1539–1542.

Kashai, E. 1958. A note on the revision of the stratigraphy of the southern Carmel. Bull. Res. Counc. Isr. 7G: 164–165.

Lewy, Z. 1989. Correlation of lithostratigraphic units in the upper Judea Group (Late Cenomanian–Late Coniacian) in Israel. Isr. J. Earth Sci. 38: 37–44.

Lipson-Benitah, S., Almogi-Labin, A., Sass, E. 1997. Cenomanian biostratigraphy and palaeoenvironments in the northwest Carmel region, northern Israel. Cretaceous Res. 18: 469–491.

Ludwig, K.R. 2000. Users manual for Isoplot/Ex version 2.3: a geochronological toolkit for Microsoft Excel. Spec. Publ. 1a, Berkeley Geochronology Center, 54 pp.

McDougall, I., Harrison, T.M. 1999. Geochronology and thermochronology by the ^{40}Ar-^{39}Ar method. Oxford University Press, New York, , 269 pp.

Picard, L., Kashai, E. 1958. On the lithostratigraphy and tectonics of the Carmel. Bull. Res. Counc. Isr. 7G: 1–19.

Renne, P.R. 1995. Excess ^{40}Ar in biotite and hornblende from the Noril'sk 1 intrusion, Siberia: implications for the age of the Siberian Traps. Earth Planet. Sci. Lett. 131: 165–176.

Roddick, J.C. 1983. High precision intercalibration of $^{40}Ar/^{39}Ar$ standards. Geochim. Cosmochim. Acta 47: 887–898.

Ron, H., Nur, A., Hofsteter, A. 1990. Late Cenozoic and recent strike slip tectonics in Mt. Carmel northern Israel, Ann. Tectonicae 4 (2): 70–80.

Sass, E. 1968. Geology of the Umm El Fahm area, northern Israel. Isr. J. Earth Sci. 17: 115–130.

Sass, E. 1980. Late Cretaceous volcanism in Mount Carmel, Israel. Isr. J. Earth Sci. 29: 8–24.

Sass, E., Bein, A. 1982, The Cretaceous carbonate platform in Israel. J. Cretaceous Res. 3: 135–144.

Segev, A. 2000. Synchronous magmatic cycles during the fragmentation of Gondwana: radiometric ages from the Levant and other provinces. Tectonophysics 325: 257–277.

Steiger, R.H., Jäger, E. 1977. Subcommission on geochronology: convention on the use of decay constants in geo- and cosmochronology. Earth Planet. Sci. Lett. 36: 359–362.

Steinitz, G., Lang, B. Mor, D., Dallal, C. 1982. The K-Ar laboratory at the Geological Survey of Israel. Geol. Surv. Isr. Curr. Res. 3: 97–99.

York, D. 1969. Least squares fitting of a straight line with correlated errors. Earth Planet. Sci. Lett. 5: 320–324.